Talanta Open 4 (2021) 100058

Contents lists available at ScienceDirect

Talanta Open

journal homepage: www.sciencedirect.com/journal/talanta-open

Spectral sensitivity of the discoloration of Historical rag paper

Yun Liu [a,b,*], Tom Fearn [c], Matija Strlič [a,b]

[a] Institute for Sustainable Heritage, University College London, Gower Street, London WC1E 6BT, UK
[b] Museum Conservation Institute, Smithsonian Institution, Museum Support Center, 4210 Silver Hill Rd, MD 20746, USA
[c] Department of Statistical Science, University College London, Gower Street, London WC1E 6BT, UK

ARTICLE INFO

Keywords:
Spectral sensitivity
Discoloration
Hyper-spectral imaging
Modelling
Paper
Cultural heritage

ABSTRACT

This paper discusses the spectral sensitivity of the discoloration of historical rag paper simultaneously affected by Relative Humidity (RH) and Oxygen concentration [O_2] in the ambient environment. Sacrificial samples were degraded using narrowband radiation sources centred at 450 nm, 525 nm, and 625 nm in combinations of RH and [O_2] at two levels: 0% [O_2] and 70% RH, 21% [O_2] and 70% RH, 0% [O_2] and 20% RH, and 21% [O_2] and 20% RH. Diffuse reflectance was measured before and during the degradation experimental runs. Consistent qualitative results were obtained for the change in reflectance and the change in tristimulus total color change in CIELAB color space. In both cases, the increase of discoloration was modelled logarithmically over time. Among the three factors investigated in this research, wavelength of the radiation (Λ) was found to have the strongest effect. The radiation at 450 nm induced the most and fastest discoloration whereas the radiation at 625 nm induced the least and slowest discoloration. This spectral dependence was likely to be related to the photo energies at different wavelengths, but other factors were found to have played a role. Further analyses revealed that the main effects and the effects of the interactions between [O_2] and Λ and between RH and Λ on the discoloration of historical rag paper were statistically significant. It suggests that managing the spectral power distribution of the radiation source can be crucial in the collection management.

List of abbreviations

ANOVA	Analysis of variance
ΔE_{00}	Total color difference defined by CIEDE2000 formula
ΔE_{00N}	Normalized total color difference defined by CIEDE2000 formula
E_v	Illuminance
$k_{\Delta E00N}$	Normalized rate constant of change in total color difference
$k_{\Delta R}$	Rate constant of change in diffuse reflectance
$k_{\Delta RN}$	Normalized rate constant of change in diffuse reflectance
$K_{\Delta RN}$	Normalized rate of change in diffuse reflectance
LED	Light-emitting diode
N	Number of photons in Mol
[O_2]	Oxygen concentration
ΔR	Change in diffuse reflectance
ΔR_N	Normalized change in diffuse reflectance
R	Diffuse reflectance
R^2	Coefficient of determination
RH	Relative humidity
SPD	Spectral power distribution
[Λ]	Narrowband radiation centered at Λ
Λ	Wavelength of radiation in nm
λ	Wavelength of reflectance in nm

1. Introduction

Managing the discoloration of collection materials is among the top priorities for museums and galleries, especially when it comes to decision making for display strategies. But this strong need has not led to sufficient scientific research on the issue. Most of the limited studies often focus on the colorants of artworks and manuscripts [21,28] with little consideration given to the supporting materials, despite the fact that the properties of substrates can affect the photochemical behavior of colorants [7–10,16]. Moreover, the discoloration of substrates has been observed to penetrate through the surface layers and significantly affect the overall measurements of discoloration of collection materials [27].

As one of the most commonly used supporting materials for art works and manuscripts, the photochemistry of paper received interest mainly in the 20th century. Experiments were designed using laboratory grade

* Corresponding author.
E-mail address: LiuY@si.edu (Y. Liu).

https://doi.org/10.1016/j.talo.2021.100058
Received 15 June 2021; Received in revised form 20 July 2021; Accepted 20 July 2021
Available online 24 July 2021

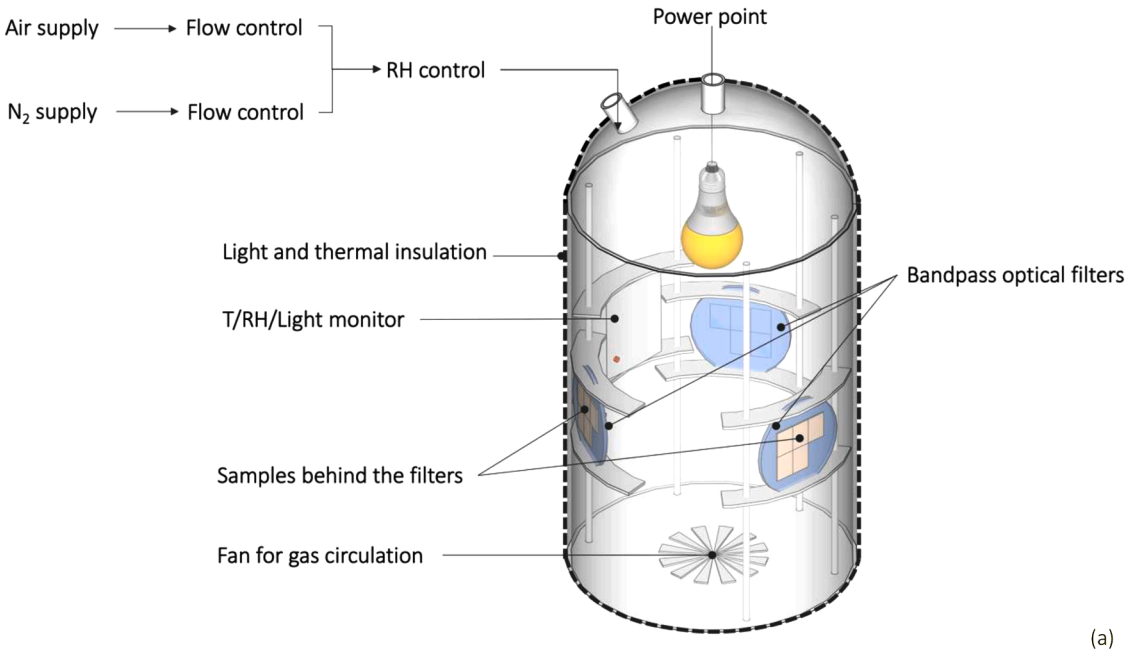

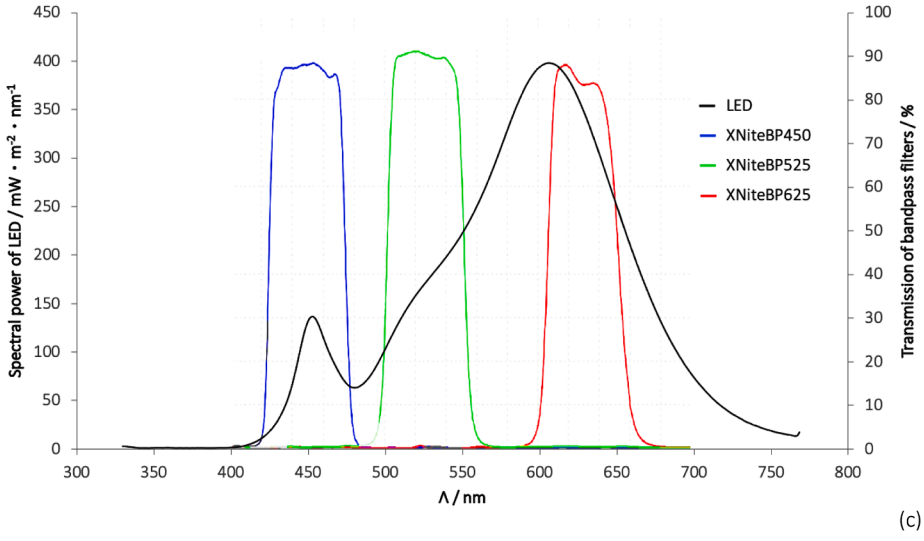

Fig. 1. (a) Diagram showing the experimental setup with environmental controls for the experiment. (b) Representation of the historical rag paper subsamples. (c) The spectral power distribution of the LED light source (black line) and the profiles of the three band-pass optical filters used in the experimental setup.

cellulose and monochrome and heterogeneous ultra violet (UV) radiation. The wavelength of radiation was found to play a decisive role in the degradation reaction kinetics [11,17,19,25]. Far and middle UV ($\lambda <$ 300 nm) was found to initiate direct photolysis, whereas near UV ($\lambda =$ 388 nm) mainly caused photo-oxidation. This observation can be explained by the fact that the energy of the photons in far and middle UV (95 kcal•mol^{-1} at 300 nm) is higher than the energy required for the scission of C-C and C-O bonds (80–90 cal•mol^{-1}) [22].

In addition to the wavelength of radiation, the effect of the moisture content of samples and the effect of the oxygen concentration of ambient environment were discussed in relation to the photochemical reaction kinetics [12–14,17]. Using UV radiation at 254 nm, where direct photolysis was the main reaction mechanism, oxygen played a small role whereas moisture strongly inhibited the degradation of cellulose, as

indicated by reflectance, degree of polymerisation, and alpha cellulose content [18]. In contrast, when UV radiation at 388 nm and heterogeneous UV radiation were used, the rate of degradation was found to increase with increasing oxygen content, as indicated by decreasing degree of polymerisation and increasing gaseous degradation products [25].

These early studies are solid and inspirational, but are not practically helpful for collection management. In the museums and archives in the Western world, concern over the discoloration of paper-based collections mostly involves the presence of iron gall ink, which is considered susceptible to fading [1]. Due to the popular use of iron gall ink before the substantial change of papermaking in the late 19th century [15], most collection items in concern are made of historical rag paper. Historical rag paper mainly contains hemp, linen and cotton fibres, gelatine sizing, and an accumulation of natural degradation products [26], which can behave differently from laboratory grade model paper. In addition, UV has been excluded in museums and archives and the Light-Emitting Diode (LED) has been commonly used for lighting [6]. The results obtained using UV radiation may not be directly applicable to today's lighting environment. Therefore, research on the discoloration of paper needs to be updated with historical rag paper and visible range of the electromagnetic spectrum in order to maximise its support for collection management.

Only a small number of research projects on the discoloration of historical paper under visible range of the electromagnetic spectrum has been carried out recently [3,20]. Liu [20] investigated the effects and interactions between Relative Humidity (RH), Oxygen concentration [O_2] and Illuminance (E_v) on Western rag paper based on factorial experimentation. Dang et al. [3] focused on the effect of different wavelengths on the discoloration of Chinese paper in a static ambient environment. It should be noted that the discoloration in the research by Dang et al. [3] was only assessed in tristimulus color space and customized colorimetric terms. This seems to be common practice in assessing discoloration of heritage collections [4,5]. Given that different formula for tristimulus color change were used in different research, transformations need to be carried out before interpreting and comparing the results.

To bridge the gaps in research on the discoloration of paper-based collections, in this research, an experiment was designed to investigate the synergistic effect of RH, oxygen and the wavelength of radiation, with an emphasis on the spectral sensitivity of the discoloration behavior. Sacrificial historical rag paper samples were used to represent the uncontrollable natural variations in the materials. Given that the tristimulus parameters are formulated based on the physiological perception of color by human vision [2,24], both spectroscopic and tristimulus responses of the samples were analyzed to examine whether consistent results could be achieved for the colorimetric study of historical rag paper. The results not only provided insights into the spectrally dependent discoloration of historical rag paper, but also have implications for museum lighting and collection management.

2. Methodology

The experiment was carried out in a reaction chamber as illustrated in Fig. 1 (a). A LED light bulb (240 V, 13 W, 1521 lm, Philips, Netherlands) was installed in the middle of the reaction chamber. The temperature (T) was constantly kept at 21°C to limit as much as possible the interference of thermal degradation during the experiment. Air and N_2 supplies were used to achieve [O_2] (v/v %) at either high (21%) or low (0%) levels respectively. Gas flows from these supplies were regulated by Aalborg GFC aluminium body mass flow controller (Caché Instrumentation, UK). The flows then passed through a V-GenTM Dew Point/RH Generator (InstruQuest Inc., US) to achieve RH at high (70%) and low (20%) levels before entering the reaction chamber. The controlled atmospheres were continuously circulated at 200 ml•min^{-1} through the system 24 h before and during the experiment.

For each experimental run, five distinct sacrificial rag paper sheets were used. These paper sheets did not have associated dates and were identified as rag paper by visual examination of the presence of sieve marks and random fibre orientations. 1.0 cm * 1.5 cm subsamples were cut from each sheet (Fig. 1 (b)) and were attached to Whatman filter paper No. 1. They were then placed behind the optical bandpass filters centred at 450 nm [Λ_{450}] (XNiteBP450, LDP LLC, US), 525 nm [Λ_{525}] (XNiteBP525, LDP LLC, US) and 625 nm [Λ_{625}] (XNiteBP625, LDP LLC, US). The spectral power distribution (SPD) of the LED light source, measured using GL SPECTIS 1.0 spectrometer (GL Optic, Poland-Germany), and the optical profiles of the filters are presented in Fig. 1 (c). The environmental condition inside the chamber was monitored using HOBO Data Loggers (U12-012, Tempcon Instrumentation, UK) at the same height as the samples in the chamber.

A total of four experimental runs were carried out in all possible combinations of the [O_2] and RH levels, i.e. 0% [O_2] and 20% RH, 0% [O_2] and 70% RH, 21% [O_2] and 20% RH, and 21% [O_2] and 70% RH. Diffuse reflectance (R) of the samples was measured before and during

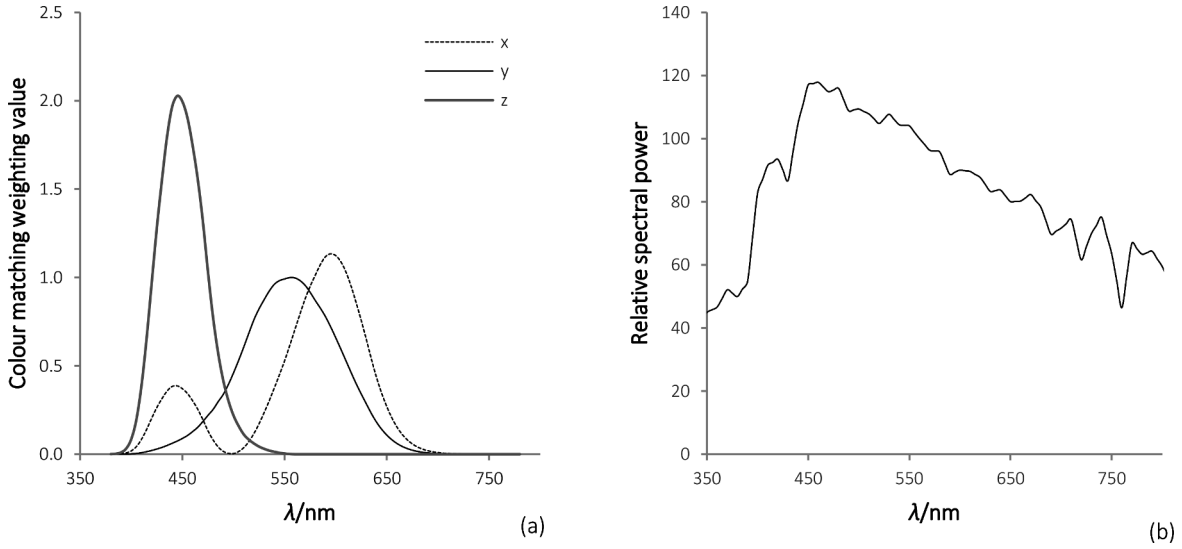

Fig. 2. (a) The distribution of color matching weighting factors for x, y and z used to calculate X, Y, and Z in CIE 1931 XYZ color space. (b) The relative SPD of the CIE Standard Illuminant D65.

the runs. For each run, it took ~1 h for the environment inside the reaction chamber to stabilise after interruption and the samples were degraded for another ~2.5 h (~0.14 day in total) to reach a measurable change in R before the first measurement was taken. Subsequent measurements were taken at intervals of 0.2–5 days until the measurements reached a plateau. The duration of the runs ranged from 11 to 30 days with at least eight data points obtained. The measurements were taken using a hyper-spectral imaging system (Camlin, Lisburn, UK). The system was equipped with a VNIR camera (spectral range: 400–1000 nm, spectral resolution: 2 nm) with an XENOPLAN 2.8/50-0902 lens (Schneider-KREVZNACH, Germany) and a halogen light source. Both dark and white calibrations were carried out before each scan at 0.8 mm•s^{-1} with 50 ms exposure time and f/5.6 aperture. The spatial resolution of the images was 625 ppi.

R of each sample was represented by the average R of all the pixels of uncontaminated paper area on that sample. For the analyses of reflectance, change in reflectance (ΔR, day^{-1}) was calculated by subtracting the reflectance spectrum before degradation from the spectrum collected at each time point. For each band-pass filter, ΔR was averaged across all the samples for each experimental condition to construct a data cube, where the first dimension was the experimental condition, the second dimension was ΔR over the reflectance spectral range (λ) of 424–853 nm, and the third dimension was the time of degradation (t). The spectra of ΔR were smoothed using Savitzky–Golay filtering (2nd order polynomial, window width 19) [23].

For the analyses of tristimulus colorimetry, R of each sample was truncated to 424–780 nm and analyzed in the CIELAB color space (Commission Internationale de l'Éclairage, abbreviated as CIE). X, Y, Z values in CIE 1931 XYZ color space were first calculated for each sample using the following equations:

$$X = n^{-1}\int x(\lambda)S(\lambda)I(\lambda)d\lambda,$$

$$Y = n^{-1}\int y(\lambda)S(\lambda)I(\lambda)d\lambda,$$

$$Z = n^{-1}\int z(\lambda)S(\lambda)I(\lambda)d\lambda,$$

$$n = \int y(\lambda)I(\lambda)d\lambda,$$

where x, y, and z are CIE 1964 standard 10 ° colorimetric observer functions which are plotted in Fig. 2 (a), S is the reflectance of the sample, I is the relative SPD of the CIE standard illumination D65 as shown in Fig. 2 (b), and n is a normalising constant. X, Y, and Z were then used to obtain L*, a*, and b* based on:

$$L* = \begin{cases} 116\left(YY_0^{-1}\right)^{1/3} - 16, & YY_0^{-1} > 0.008856 \\ 903.3\left(YY_0^{-1}\right), & YY_0^{-1} \le 0.008856 \end{cases},$$

$$a* = 500\left(f\left(XX_0^{-1}\right) - f\left(YY_0^{-1}\right)\right),$$

$$b* = 200\left(f\left(YY_0^{-1}\right) - f\left(ZZ_0^{-1}\right)\right),$$

where $(k) = \begin{cases} k^{1/3}, & k > 0.008856 \\ 7.787k + 16/116, & k \le 0.008856 \end{cases}$, X_0, Y_0 and Z_0 are the tristimulus values of the reference white for the CIE standard Illuminant D50. Based on these calculations, the total color change of each historical rag paper sample (ΔE_{00}) was calculated using the formula given by CIE [2,24] at each time a measurement was taken. ΔE_{00} was then average across all the samples degraded under the same condition for further analyses. All the data analyses were carried out in MATLAB® R2017a.

Table 1
The normalized rate constant of change in diffuse reflectance ($k_{\Delta RN}$) of historical rag paper at sampled λ in different conditions. The results for (a) [Λ_{450}], (b) [Λ_{525}], and (c) [Λ_{625}] are presented in separate tables for comparison. λ is the wavelength of measured reflection in nm, $k_{\Delta RN}$ is in mol^{-1}. R^2 represents the goodness-of-fit of the logarithmic models based on Equation 3 and 4.

(a) [Λ_{450}]

λ/nm	0% [O_2], 70% RH		21% [O_2], 70% RH		0% [O_2], 20% RH		21% [O_2], 20% RH	
	$k_{\Delta RN\text{-}B}$	R^2	$k_{\Delta RN\text{-}B}$	R^2	$k_{\Delta RN\text{-}B}$	R^2	$k_{\Delta RN\text{-}B}$	R^2
424	6.11 × 10^{-7}	0.91	6.23 × 10^{-7}	0.87	2.0 × 10^{-7}	0.62	3.22 × 10^{-7}	0.75
444	4.32 × 10^{-7}	0.95	3.87 × 10^{-7}	0.93	1.34 × 10^{-7}	0.94	2.71 × 10^{-7}	0.95
497	2.83 × 10^{-7}	0.89	2.00 × 10^{-7}	0.80	5.07 × 10^{-8}	0.68	1.43 × 10^{-7}	0.90
549	1.70 × 10^{-7}	0.67	5.36 × 10^{-8}	0.20	0.00	0.00	6.85 × 10^{-8}	0.54
601	1.19 × 10^{-7}	0.41	-2.98 × 10^{-8}	0.06	-1.79 × 10^{-8}	0.15	-5.96 × 10^{-9}	0.02
654	9.54 × 10^{-8}	0.26	-6.85 × 10^{-8}	0.21	-2.68 × 10^{-8}	0.25	-3.58 × 10^{-8}	0.36
706	7.75 × 10^{-8}	0.18	-8.94 × 10^{-8}	0.27	-3.87 × 10^{-8}	0.34	-5.66 × 10^{-8}	0.55
758	5.96 × 10^{-8}	0.12	-9.54 × 10^{-8}	0.28	-4.77 × 10^{-8}	0.38	-7.15 × 10^{-8}	0.62
811	5.66 × 10^{-8}	0.10	-9.54 × 10^{-8}	0.25	-5.66 × 10^{-8}	0.40	-8.05 × 10^{-8}	0.61
853	5.07 × 10^{-8}	0.08	-9.84 × 10^{-8}	0.24	-5.96 × 10^{-8}	0.37	-8.64 × 10^{-8}	0.60

(b) [Λ_{525}]

λ/nm	0% [O_2], 70% RH		21% [O_2], 70% RH		0% [O_2], 20% RH		21% [O_2], 20% RH	
	$k_{\Delta RN\text{-}G}$	R^2	$k_{\Delta RN\text{-}G}$	R^2	$k_{\Delta RN\text{-}G}$	R^2	$k_{\Delta RN\text{-}G}$	R^2
424	1.38 × 10^{-7}	0.70	2.07 × 10^{-7}	0.83	×	0.02	5.44 × 10^{-8}	0.42
444	1.06 × 10^{-7}	0.91	1.41 × 10^{-7}	0.94	2.72 × 10^{-8}	0.81	7.77 × 10^{-8}	0.92
497	9.06 × 10^{-8}	0.92	1.14 × 10^{-7}	0.96	2.72 × 10^{-8}	0.83	7.25 × 10^{-8}	0.95
549	4.92 × 10^{-8}	0.77	6.21 × 10^{-8}	0.85	7.77 × 10^{-9}	0.30	4.92 × 10^{-8}	0.79
601	1.81 × 10^{-8}	0.24	2.20 × 10^{-8}	0.36	-6.47 × 10^{-9}	0.19	3.88 × 10^{-9}	0.07
654	0.00	0.00	2.59 × 10^{-9}	0.01	-1.16 × 10^{-8}	0.40	-1.29 × 10^{-8}	0.37
706	-1.16 × 10^{-8}	0.08	-7.77 × 10^{-9}	0.03	-1.55 × 10^{-8}	0.48	-2.20 × 10^{-8}	0.57
758	-2.20 × 10^{-8}	0.25	-1.29 × 10^{-8}	0.08	-1.81 × 10^{-8}	0.51	-2.98 × 10^{-8}	0.62
811	-2.72 × 10^{-8}	0.30	-1.42 × 10^{-8}	0.09	-2.07 × 10^{-8}	0.51	-3.24 × 10^{-8}	0.60
853	-3.11 × 10^{-8}	0.31	-1.68 × 10^{-8}	0.11	-2.20 × 10^{-8}	0.50	-3.49 × 10^{-8}	0.57

(c) [Λ_{625}]

λ/nm	0% [O_2], 70% RH		21% [O_2], 70% RH		0% [O_2], 20% RH		21% [O_2], 20% RH	
	$k_{\Delta RN\text{-}R}$	R^2	$k_{\Delta RN\text{-}R}$	R^2	$k_{\Delta RN\text{-}R}$	R^2	$k_{\Delta RN\text{-}R}$	R^2
424	3.71 × 10^{-8}	0.51	6.61 × 10^{-8}	0.73	3.23 × 10^{-9}	0.03	2.31 × 10^{-8}	0.37
444	3.44 × 10^{-8}	0.76	3.71 × 10^{-8}	0.92	8.60 × 10^{-9}	0.82	1.56 × 10^{-8}	0.66
497	2.96 × 10^{-8}	0.73	2.96 × 10^{-8}	0.93	7.53 × 10^{-9}	0.64	1.56 × 10^{-8}	0.67
549		0.60		0.87		0.47		0.68

(continued on next page)

Table 1 (*continued*)

(c) [Λ_{625}] λ/nm	0% [O_2], 70% RH $k_{\Delta RN-R}$	R^2	21% [O_2], 70% RH $k_{\Delta RN-R}$	R^2	0% [O_2], 20% RH $k_{\Delta RN-R}$	R^2	21% [O_2], 20% RH $k_{\Delta RN-R}$	R^2
	2.31×10^{-8}		2.15×10^{-8}		7.53×10^{-9}		1.67×10^{-8}	
601	1.61×10^{-8}	0.40	1.24×10^{-8}	0.62	5.38×10^{-9}	0.23	3.76×10^{-9}	0.09
654	9.14×10^{-9}	0.17	5.92×10^{-9}	0.21	3.23×10^{-9}	0.06	-3.23×10^{-9}	0.06
706	3.76×10^{-9}	0.03	1.61×10^{-9}	0.02	1.61×10^{-9}	0.01	-8.07×10^{-9}	0.29
758	-5.38×10^{-10}	0.00	-1.08×10^{-9}	0.00	5.38×10^{-10}	0.00	-1.13×10^{-8}	0.42
811	-2.15×10^{-9}	0.01	-1.08×10^{-9}	0.00	0.00	0.00	-1.29×10^{-8}	0.45
853	-3.76×10^{-9}	0.02	-1.61×10^{-9}	0.01	0.00	0.00	-1.40×10^{-8}	0.45

3. Results and discussion

3.1. Spectral colorimetric change

Given that the monochrome light sources were generated using band-pass filters with a broadband LED radiation source with non-uniform spectral power distribution (Fig. 1 (c)), ΔR was normalized by the number of photons that reached the samples. The number of photons (N, mol) was calculated based on the Planck-Einstein relation:

$$N = \Lambda E(N_A hc)^{-1}, \quad (1)$$

where Λ is the wavelength of the radiation in nm, E is the total photon energy reached the sample surface in $J \cdot s^{-1} \cdot m^{-2}$, N_A is Avogadro's constant in mol^{-1}, h is Planck constant in J•s, and c is the speed of light in vacuum in $m \cdot s^{-1}$. E was measured using GL SPECTIS 1.0 (GL Optic, Poland-Germany) at the positions of the samples in the reaction chamber. Under the assumption that the number of photons absorbed and induced the discoloration of the samples was proportional to the number of photons incident on the samples, the normalized change in reflectance (ΔR_N) for each light source [Λ] was calculated as:

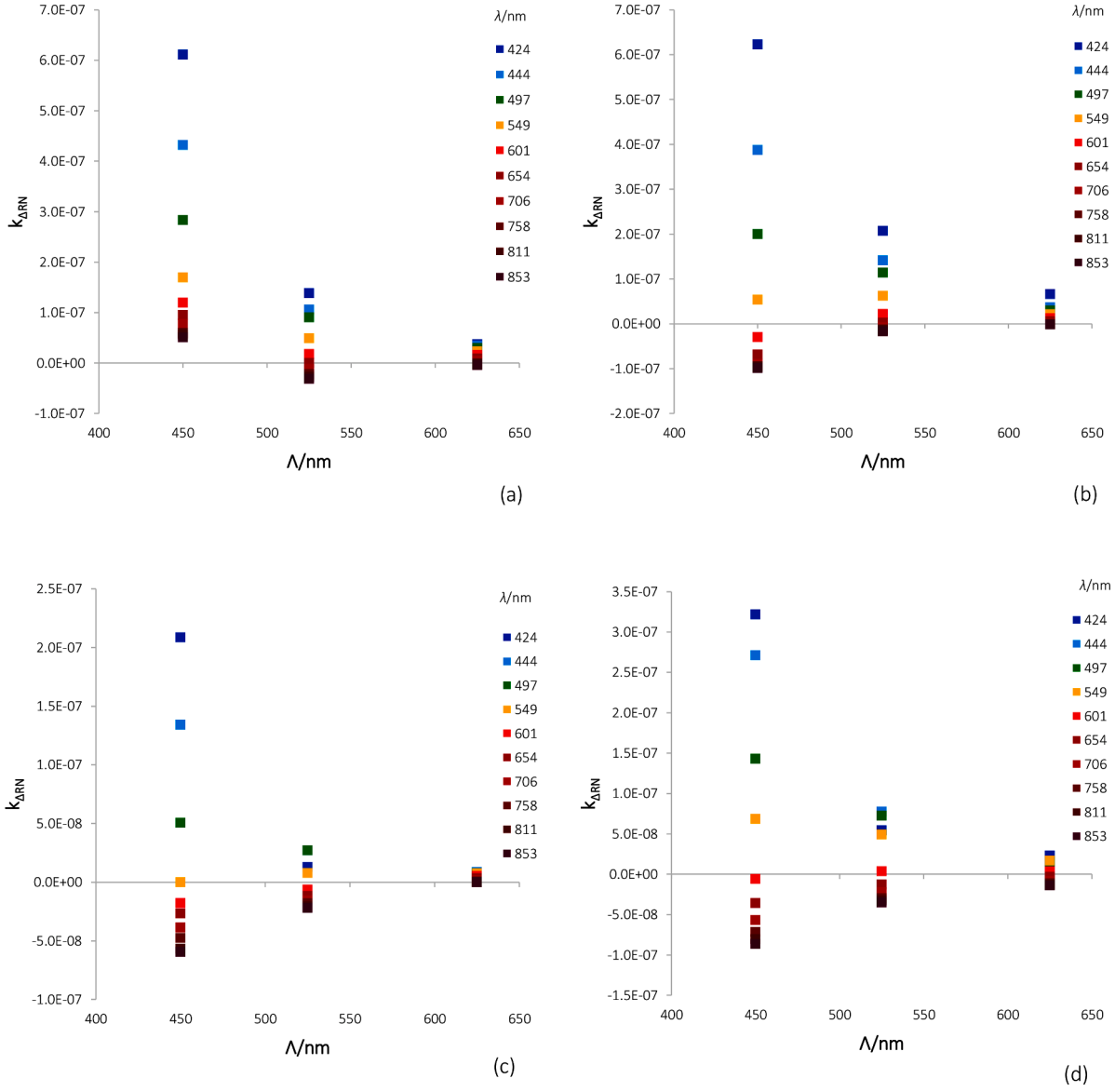

Fig. 3. Scatter plots showing the dependence of kΔRN on Λ in four experimental conditions: (a) 0% [O_2] and 70% RH, (b) 21% [O_2] and 70% RH, (c) 0% [O_2] and 20% RH, and (d) 21% [O_2] and 20% RH.

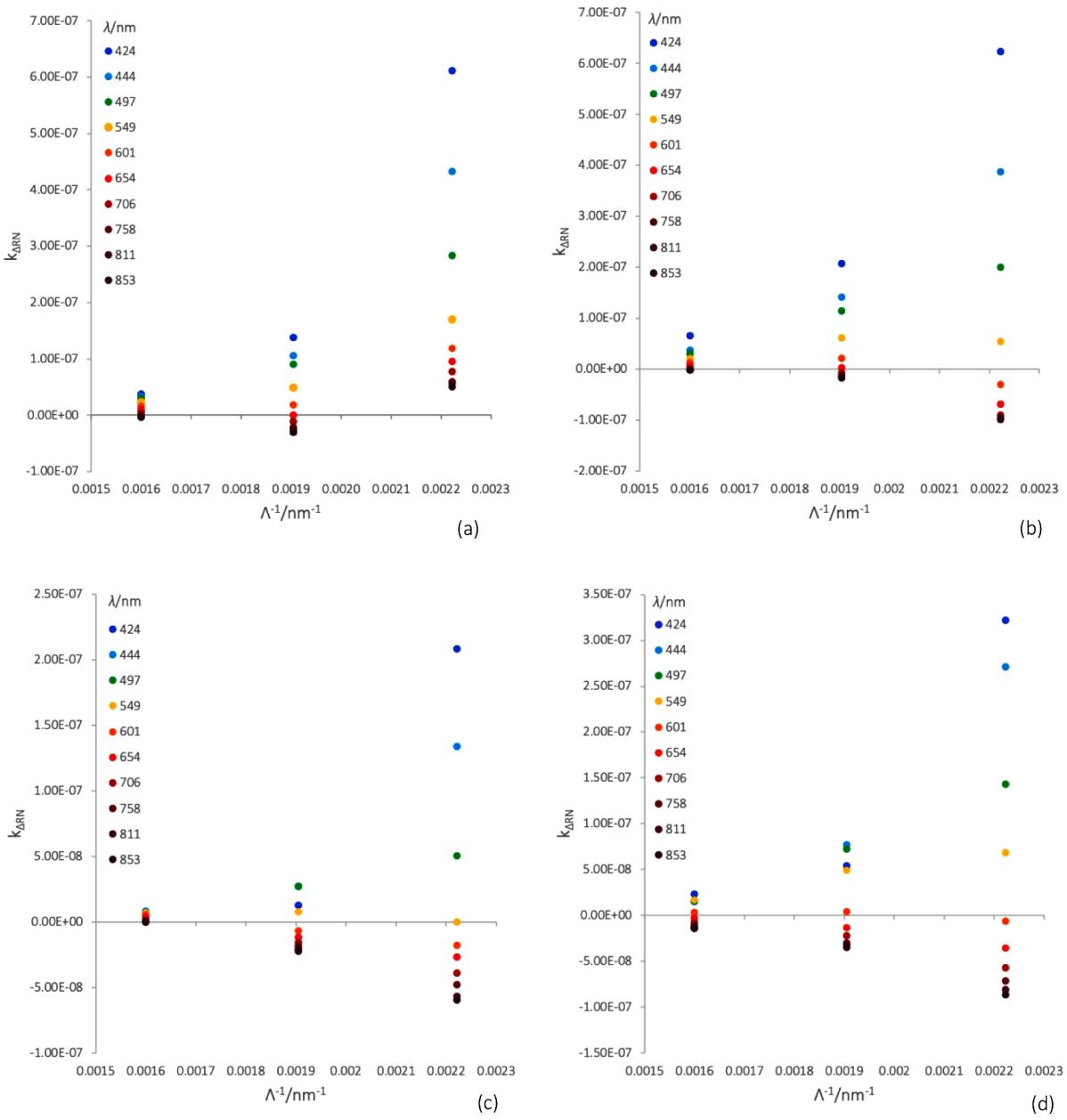

Fig. 4. Scatter plots showing the dependence of $k_{\Delta RN}$ on Λ^{-1} in four experimental conditions: (a) 0% [O_2] and 70% RH, (b) 21% [O_2] and 70% RH, (c) 0% [O_2] and 20% RH, and (d) 21% [O_2] and 20% RH.

$$\Delta R_N = N^{-1}\Delta R. \quad (2)$$

The progression of ΔR_N over time (t/day^{-1}) followed a logarithmic pattern. This is similar to the behavior of historical rag paper irradiated by a broadband LED light source, which has been discussed in detail by Liu [20]. Therefore, a similar modelling approach was taken, where the relationship between ΔR_N and t was modelled using a logarithmic relationship:

$$\Delta R_N = \begin{cases} 0, & t = 0 \\ A_0 + k_{\Delta RN}\ln t, & t \geq 0.14 \end{cases}, \quad (3)$$

where A_0 is the normalized amount of spectral change took place in one day, the first measurement was taken at t = 0.14 day, and $k_{\Delta RN}$ is the rate constant of the normalized rate of spectral change ($K_{\Delta RN}$) derived according to the following equations:

$$K_{\Delta RN} = \begin{cases} 0, & t = 0 \\ d\Delta R_N(dt)^{-1} = k_{\Delta RN}t^{-1}, & t \geq 0.14 \end{cases}. \quad (4)$$

Based on these four equations, $k_{\Delta RN}$ was calculated over 424–853 nm at approximately 50 nm intervals for the samples exposed to [Λ_{450}] ($k_{\Delta RN\text{-}B}$), [Λ_{525}] ($k_{\Delta RN\text{-}G}$) and [Λ_{625}] ($k_{\Delta RN\text{-}R}$). The results are summarized in Table 1. The results show that all the light sources induced changes of the samples in reflectance across 424–853 nm. Similar to the effect of the broadband radiation [20], $k_{\Delta RN\text{-}B}$, $k_{\Delta RN\text{-}G}$, and $k_{\Delta RN\text{-}R}$ decreased as λ increased with positive maxima reached at the short end of the λ range. $k_{\Delta RN\text{-}B}$, $k_{\Delta RN\text{-}G}$, and $k_{\Delta RN\text{-}R}$ obtained at high RH were generally higher than those obtained at low RH, suggesting that RH was likely to play a positive role in driving the rate of discoloration of historical rag paper. It should be noted that $k_{\Delta RN}$ is generally positive when λ < 600 nm and negative when λ > 600 nm. This indicates that R increased at short wavelengths and decreased at long wavelengths, which led to blue-shift of the reflectance spectra as the samples degraded. It should also be noted that $k_{\Delta RN\text{-}B}$, $k_{\Delta RN\text{-}G}$, and $k_{\Delta RN\text{-}R}$ are much smaller than the rate constant obtained with broadband radiation using the same experimental setup [20]. This suggests that the signal to

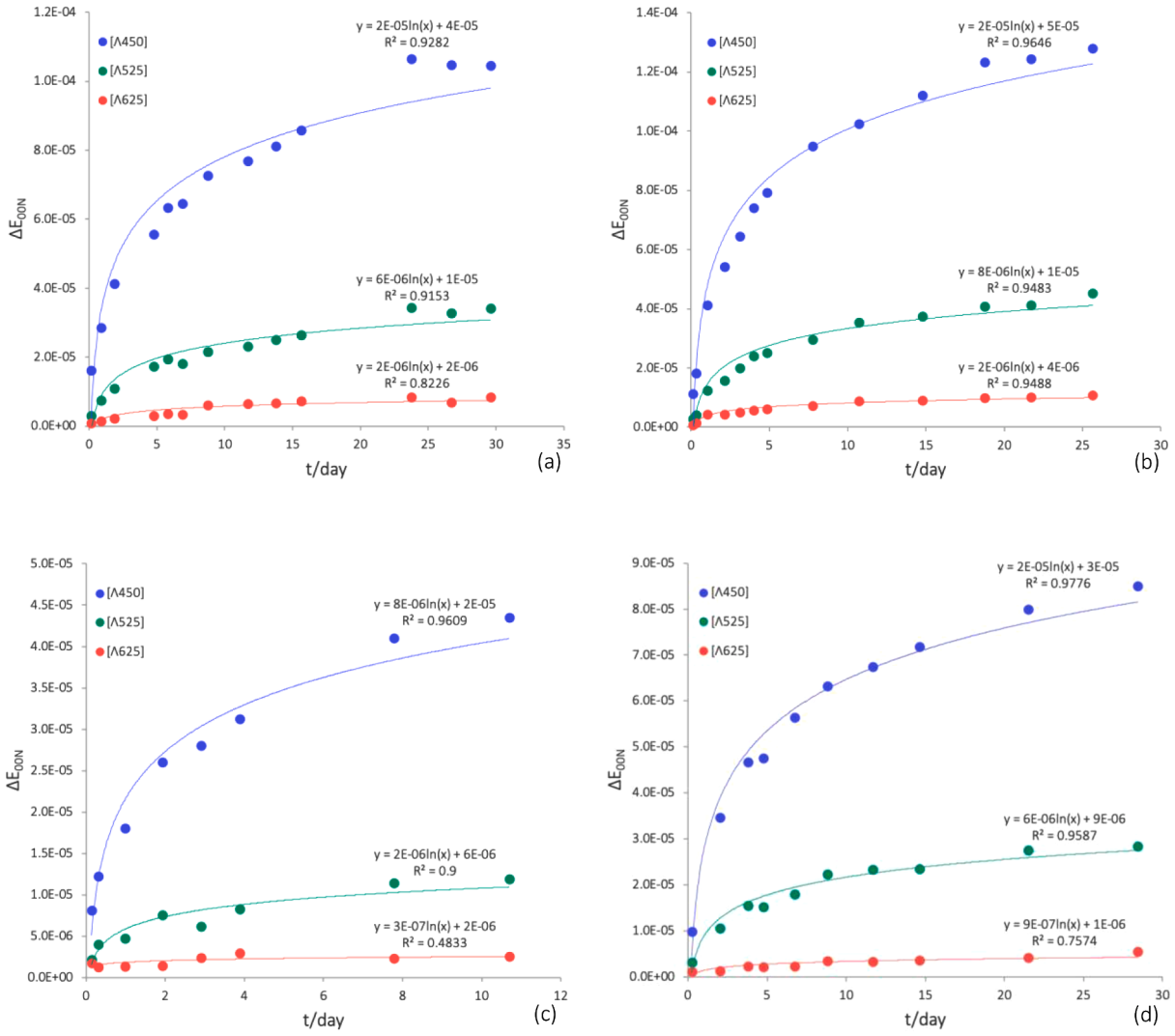

Fig. 5. Scatter plots showing the progression of ΔE_{00N} of paper samples exposed to [Λ_{450}], [Λ_{525}]and [Λ_{625}] over time under different combinations of [O_2] and RH: (a) 0% [O_2] and 70% RH, (b) 21% [O_2] and 70% RH, (c) 0% [O_2] and 20% RH, and (d) 21% [O_2] and 20% RH. The relationship was approximated using linear trend lines with high goodness-of-fit.

noise ratio was likely to be relatively lower in this research. For the even smaller $k_{\Delta RN}$ obtained at $\lambda > 600$ nm, where the data scatter was also larger, the effective spectral change was likely to be un-measurable and the values mainly represented noise.

To elucidate the wavelength dependence of the spectral changes, the relationship between $k_{\Delta RN}$ and Λ was explored as shown in Fig. 3. It clearly shows that under all the combinations of [O_2] and RH, [Λ_{450}] induced the fastest changes across 424–853 nm whereas [Λ_{625}] induced the slowest. On average, $k_{\Delta RN\text{-}B}$ was found ~12 times as much as $k_{\Delta RN\text{-}R}$ and ~3 times as much as $k_{\Delta RN\text{-}G}$ across different environmental conditions. This is likely to be an effect of the higher energy carried by the photons of 450 nm than the photons of 625 nm. Given that the relationship between photon energy (E) and Λ is reciprocal according to this equation:

$$E = hc\Lambda^{-1}, \tag{5}$$

the relationship between $k_{\Delta RN}$ and Λ^{-1} was further plotted, as shown in Fig. 4. Nonlinearity was observed between $k_{\Delta RN}$ and Λ^{-1} at the selected λ in different conditions, with the possibility of linearity at a certain λ. This indicates that photon energy alone is insufficient to explain the observed changes and there were other factors that affected the discoloration of historical rag paper in the experiment. However, it is beyond the scope of this research to investigate these factors where additional experiments need to be designed and measurements of higher resolution need to be obtained.

3.2. *Tristimulus total color change*

For the management of discoloration of historical rag paper in practice, it is essential to understand the relationship between the spectral response and the physiological perception of color by humans. To investigate if tristimulus colorimetric assessment was in agreement with the measurements of spectral responses of historical rag paper, tristimulus total color change ΔE_{00} in the CIELAB color-space was calculated as described in detail in Methodology. Similar to the normalisation of ΔR, normalized ΔE_{00} (ΔE_{00N}) was achieved by dividing ΔE_{00} by the number of photons N (Equation 1) as:

$$\Delta E_{00N} = N^{-1}\Delta E_{00}. \tag{6}$$

The progression of ΔE_{00N} over time is presented in Fig. 5. Across all the experimental conditions, ~50% of the total color change of the samples was completed in the first five days. Similar to the observations made for reflectance, the effect of [Λ] on ΔE_{00N} decreased as Λ increased. [Λ_{450}] induced remarkably faster and larger change in ΔE_{00N}, which was likely to be associated with the higher energy of photons of

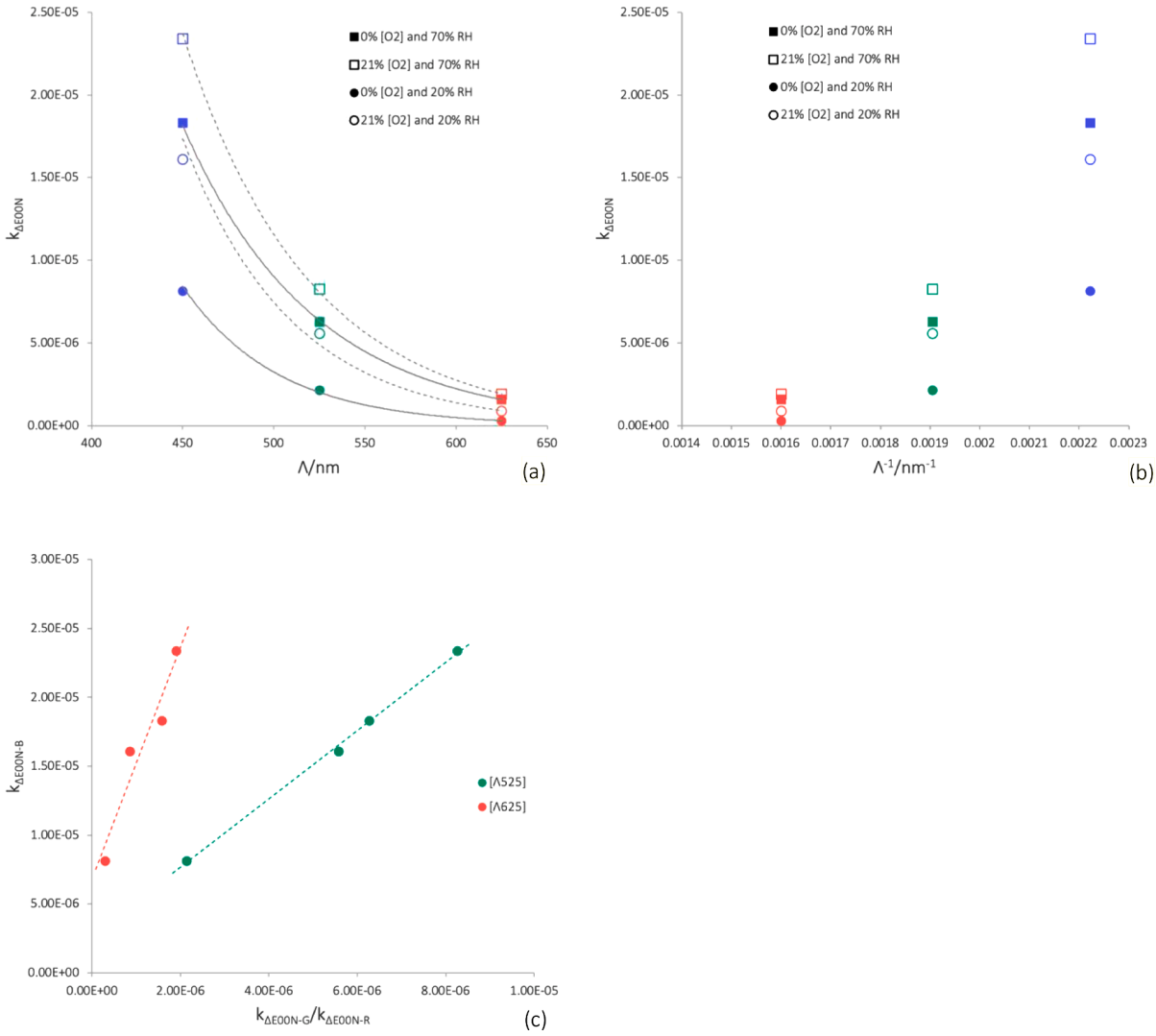

Fig. 6. (a) Plots showing the dependence of $k_{\Delta E00N}$ on Λ in different environmental conditions. The relationship was approximated using exponential trend lines with high goodness-of-fit. (b) Plots showing the relationships between $k_{\Delta E00N}$ and Λ^{-1}. (c) Plots showing the relationship between $k_{\Delta E00N\text{-}B}$ and $k_{\Delta E00N\text{-}G}$ (green) and between $k_{\Delta E00N\text{-}B}$ and $k_{\Delta E00N\text{-}R}$ (red) across different environmental conditions.

450 nm than the photons of 625 nm. Based on Equations 3 and 4, the progression of ΔE_{00N} induced by $[\Lambda_{450}]$, $[\Lambda_{525}]$ and $[\Lambda_{625}]$ over time was approximated using a logarithmic relationship. The rate constant of change in ΔE_{00N} ($k_{\Delta E00N}$) was obtained as the pre-logarithmic coefficient as indicated in Fig. 5. The sufficiency of the logarithmic approximation was indicated by the high goodness-of-fit (R^2).

Table 2
ANOVA for the effects of $[O_2]$, RH, Λ and their interactions on logarithmic $k_{\Delta E00N}$.

Source	Sum of squares	Degree of freedom	Mean square	F-value	*p*-value
$[O_2]$	0.98	1	0.98	120.37	3.92E-04
RH	2.21	1	2.21	271.11	7.97E-05
Λ	15.97	1	15.97	1955.22	1.56E-06
$[O_2]$*RH	0.34	1	0.34	41.75	2.96E-03
$[O_2]$*Λ	0.01	1	0.01	1.62	2.72E-01
RH*Λ	0.23	1	0.23	27.69	6.25E-03
$[O_2]$ *RH*Λ	0.03	1	0.03	3.23	1.47E-01
Residuals	0.03	4	0.01		

The dependence of $k_{\Delta E00N}$ on Λ was investigated and illustrated in Fig. 6 (a). The relationship seemed to follow part of an exponential or a hyperbolic curve. Given the relationship between photon energy and Λ as described in Equation 5, the relationship between $k_{\Delta E00N}$ and Λ^{-1} was investigated as shown in Fig. 6 (b). Gentle curvature in this relationship was observed across the environmental conditions, which suggests that the relationship between $k_{\Delta E00N}$ and photon energy of the light sources was not linear. This is consistent with what was observed for the spectral response. It indicates that for historical rag paper, the tristimulus compression and transformation of the spectral change did not seem to cause loss of qualitative information. This provides evidence of plausibility to use tristimulus colorimetry to qualitatively monitor the discoloration of historical rag paper in practice.

However, the tristimulus transformation was found to have quantitative impact on the results obtained by reflectance spectrometry. To reveal the impact, the relationship between $k_{\Delta E00N\text{-}B}$, $k_{\Delta E00N\text{-}G}$ and $k_{\Delta E00N\text{-}R}$ was examined and is shown in Fig. 6 (c). Linearity was observed across the four environmental conditions. $k_{\Delta E00N\text{-}B}$ was about 2.5 times and 8.5 times as much as $k_{\Delta E00N\text{-}G}$ and $k_{\Delta E00N\text{-}R}$ respectively. These

coefficients of proportionality are not equal to those obtained by the spectroscopic measurements ($k_{\Delta RN}$) as discussed before. The relative power of effect between [Λ_{450}] and [Λ_{525}] was found similar between the spectroscopic and the tristimulus assessments, whereas the relative power of effect between [Λ_{450}] and [Λ_{625}] was shrank by 35% by the tristimulus transformation.

Furthermore, a closer look at Fig. 6 (a) reveals that faster discoloration took place when RH was high. At the same RH level, faster total color change was observed at higher [O_2]. This suggests that both RH and [O_2] promoted the total color change of historical rag paper. This observation is consistent with the discoloration behavior of historical rag paper induced by broadband radiation [20] and the discoloration of cellulose irradiated by near UV [25]. Based on this observation, the effects of [O_2], RH, Λ and their interactions on logarithmic $k_{\Delta E00N}$ were further analyzed by analysis of variance (ANOVA) and a summary of the results is presented in Table 2. The results of ANOVA provided supporting evidence that all of [O_2], RH and Λ affected the discoloration of historical rag paper. Within the range of the factors investigated in the experiment, the main effects were found significantly strong with Λ showed the strongest effect. The interaction between [O_2] and Λ and between RH and Λ were also found significant. It suggests that [O_2], RH, Λ, [O_2]*Λ and RH* Λ need to be given attention in the management of discoloration of historical rag paper. In particular, controlling the SPD of light sources can be crucial in controlling the rate and the amount of discoloration.

4. Conclusions

This paper discussed the wavelength dependent discoloration of historical rag paper simultaneously affected by [O_2] and RH. Narrowband monochrome light sources centred at 450 nm, 525 nm, and 625 nm were used. The results obtained in normalized diffuse reflectance and tristimulus total color change were discussed and compared. The compression and transformation of tristimulus analyses of the spectral data was not found to cause loss of qualitative information regarding the progression of discoloration over time and the relative strength of the effect of [O_2], RH and Λ. This provides scientific evidence to support the use of tristimulus colorimetry as a way to qualitatively monitor the discoloration of rag paper-based collections in practice.

The progression of change in both diffuse reflectance and total color change over time was modelled using a logarithmic relationship and the normalized rate constant, $k_{\Delta RN}$ and $k_{\Delta E00N}$, were obtained. In both cases, Λ was observed to have the strongest effect on the rate constant, where $k_{\Delta RN}$ and $k_{\Delta E00N}$ decreased as Λ increased. [O_2] and RH were observed to have promoted the discoloration. This suggests that lowering [O_2], RH, and the proportion of short wavelengths in the light source can be a practical management strategy to control the discoloration of historical rag paper-based collections. ANOVA confirmed these results and additionally revealed that the interactions between [O_2] and Λ and between RH and Λ were also significant. This reinforces that the spectral power distribution of light sources plays an important role in affecting the discoloration of historical rag paper. However, all of [O_2], RH, Λ, [O_2]*Λ and RH*Λ need to be monitored and assessed in the collection management to achieve the best outcome.

For $k_{\Delta RN}$, [Λ_{450}] induced about twice faster discoloration than that induced by [Λ_{525}] and more than 10 times faster response than that induced by [Λ_{625}]. For $k_{\Delta E00N}$, [Λ_{450}] induced ~1.5 times faster discoloration than that induced by [Λ_{525}] and ~7.5 times faster response than that induced by [Λ_{625}]. The discrepancy in the coefficients of proportionality between $k_{\Delta RN}$ and $k_{\Delta E00N}$ suggests that the tristimulus transformation caused quantitative distortion of the spectral assessments and may not be used for quantitative assessment of the spectrally dependent discoloration of historical rag paper in collection management. The coefficients of proportionality are likely to be associated with the higher energy carried by photons of 450 nm than photons of 525 nm and photons of 625 nm. Since the coefficients of proportionality were not equal to that of the photon energies, other factors related to λ and Λ were likely to have played significant roles in the discoloration processes of historical rag paper.

Declarations

Availability of data and materials: The datasets used and/or analyzed during the current study are available from the corresponding author on reasonable request. Funding: This research was generously supported by the Engineering and Physical Sciences Research Council (EPSRC) Centre for Doctoral Training in Science and Engineering in Arts, Heritage and Archaeology (SEAHA), UK and the Smithsonian's Museum Conservation Institute Trust Funds, USA. Acknowledgements: The authors would like to acknowledge the support by UCL Institute for Sustainable Heritage (UK), the Smithsonian's Museum Conservation Institute (USA), The National Archives (UK) and Lichtblau e.K. (Germany). Author contributions: Y. L., T. F. and M. S. jointly designed the experiment. Y. L. carried out all the experimental runs and data analysis. All the authors discussed the results and contributed to the manuscript. Competing interests: The authors declare that they have no competing interests.

References

[1] BSI, Specification for Managing Environmental Conditions for Cultural Collections PAS 198:2012 (2012) 2012.
[2] CIE, Improvement to Industrial Color-Difference Evaluation, Comission Internationale de L'Éclairage, 2001. Vinenna.
[3] R. Dang, et al., Spectral damage model for lighting paper and silk in museum, J. Cult. Heritage 45 (2020) 249–253, https://doi.org/10.1016/j.culher.2020.03.001.
[4] A. Fenech, et al., Modelling the lifetime of color photographs in archival collections, Stud. Conserv. 58 (2) (2013) 107–116, https://doi.org/10.1179/2047058412Y.0000000081.
[5] B. Ford, The accelerated light fading of iron gall inks in air, hypoxia and near-anoxia, in: ICOM-CC 17th Triennial Conference Preprints, 2014, p. 0604 (iii), p. art.
[6] D. Garside, et al., How is museum lighting selected? An insight into current practice in UK museums, J. Inst. Conserv.. Taylor & Francis 40 (1) (2017) 3–14, https://doi.org/10.1080/19455224.2016.1267025.
[7] C. Gervais, et al., Why does Prussian blue fade? understanding the role(s) of the substrate, J. Anal. At. Spectrom. 28 (10) (2013) 1600–1609, https://doi.org/10.1039/c3ja50025j.
[8] C. Gervais, et al., Light and anoxia fading of Prussian blue dyed textiles, Heritage Sci. 2 (1) (2014) 2–9, https://doi.org/10.1186/s40494-014-0026-x.
[9] C. Gervais, et al., X-ray photo-chemistry of Prussian blue cellulosic materials: evidence for a substrate-mediated Redox Process, Langmuir 31 (29) (2015) 8168–8175, https://doi.org/10.1021/acs.langmuir.5b00770.
[10] C. Gervais, et al., Time resolved XANES illustrates a substrate-mediated redox process in Prussian blue cultural heritage materials, J. Phys. Conf. Ser. 712 (1) (2016) 4–8, https://doi.org/10.1088/1742-6596/712/1/012139.
[11] N.-S. Hon, Formation of free radicals in photo-irradiated cellulose. I. effect of wavelength, J. Polym. Sci.: Polym. Chem. Ed. 13 (1975) 1347–1361.
[12] N.-S. Hon, Formation of free radicals in photo-irradiated Cellulose. II. effect of moisture, J. Polym. Sci.: Polym. Chem. Ed. 13 (1975) 955–959.
[13] N.-S. Hon, Formation of free radicals in photo-irradiated Cellulose. VI. effect of Lignin, J. Polym. Sci.: Polym. Chem. Ed. 13 (1975) 2641–2652.
[14] N.-S. Hon, Fundamental degradation processes relevant to solar irradiation of cellulose: ESR studies, J. Macromol. Sci.: Part A - Chem. 10 (6) (1976) 1175–1192, https://doi.org/10.1080/00222337608061243.
[15] D. Hunter, Papermaking: The History and Technique of an Ancient Craft, Courier Corporation, 1978.
[16] D. Koestler, et al., Does argon anoxia cause a color change in Prussian blue pigment? J. Am. Inst. Conserv. Taylor & Francis 57 (1–2) (2018) 47–61, https://doi.org/10.1080/01971360.2018.1478534.
[17] C. Kujirai, Studies on the photo-degradation of cellulose (IV) Infrared absorption spectra of irradiated samples (V) On the formation of cellulose peroxide, SEN-I GAKKAISHI 21 (12) (1965) 626–634.
[18] H.F. Launer, W.K. Wilson, Photochemical stability of papers, J. Res. Natl. Bur. Stand. A B 30 (1943) 55–74.
[19] H.F. Launer, W.K. Wilson, The photo-chemistry of cellulose. effects of water vapor and Oxygen in the far and near ultraviolet regions, J. Am. Chem. Soc. 71 (3) (1949) 958–962, https://doi.org/10.1021/ja01171a054.
[20] Y. Liu. Dose-response modelling for degradation of historical paper containing iron gall ink, Doctoral thesis (Ph.D.), UCL (University College London), 2019.
[21] K. McLaren, The spectral regions of daylight which cause fading, Color. Technol. 72 (3) (1956) 86–99, https://doi.org/10.1063/1.460797.
[22] G.O. Phillips, Photochemistry of carbohydrates, Adv. Carbohydrate Chem. Acad. Press 18 (1963) 9–59, https://doi.org/10.1016/S0096-5332(08)60239-8.

[23] A. Savitzky, M.J.E. Golay, Smoothing and Differentiation of Data by Simplified Least Squares Procedures, Anal. Chem. 36 (8) (1964) 1627–1639, https://doi.org/10.1021/ac60214a047.
[24] G. Sharma, W. Wu, E.N. Dalal, The CIEDE2000 color-difference formula: implementation notes, supplementary test data, and mathematical observations, Color Res. App. 30 (1) (2005) 21–30, https://doi.org/10.1002/col.20070.
[25] R.A. Stillings, R.J. Van Nostrand, The action of ultra-violet light upon cellulose. I. irradiation effects. II. Post-Irradiation Effects 1, J. Am. Chem. Soc. 66 (5) (1944) 753–760, https://doi.org/10.1021/ja01233a029.
[26] M. Strlič, et al., Development and mining of a database of historic European paper properties, Cellulose 27 (14) (2020) 8287–8299, https://doi.org/10.1007/s10570-020-03344-x.
[27] J. Thomas, et al., A chemi-luminescence study of madder lakes on paper, Polym. Degrad. Stab. 95 (12) (2010) 2343–2349, https://doi.org/10.1016/j.polymdegradstab.2010.08.024.
[28] P.M. Whitmore, X. Pan, C. Bailie, Predicting the fading of objects: identification of fugitive colorants through direct non-destructive light-fastness measurements, J. Am. Inst. Conserv. 38 (3) (1999) 395–409, https://doi.org/10.1179/019713699806113420.